Karlsruher Institut für Technologie

Institute for Structural Analysis
Head of the Institute:
Prof. Dr.-Ing. S. Freitag

Numerical design analysis and experimental investigation of multichamber soft fluidic actuators for omnidirectional gripping applications

Maximilian Pawlik

1. Objectives and backgrounds

In recent years, robotic applications have become increasingly relevant for fine motor operations. Advances in soft materials have driven the emergence of soft robotics, encompassing a broad range of actuation technologies. Among these, soft fluidic actuators (SFAs) are particularly prominent. Operated pneumatically or hydraulically, they enable low-energy deformation with minimal geometric constraints. To capture an SFA's diverse deformation modes, numerical simulations are indispensable. Their validity must be demonstrated experimentally so that the resulting analytical data can be utilised in control algorithms.

2. A SFA's single-chamber model

The simplest SFA design consists of four silicone-rubber membranes of thickness t_0, arranged in a rectangular configuration enclosing a single chamber (Figure 1). One end of the actuator is clamped, while the opposite end is sealed by a fifth membrane.

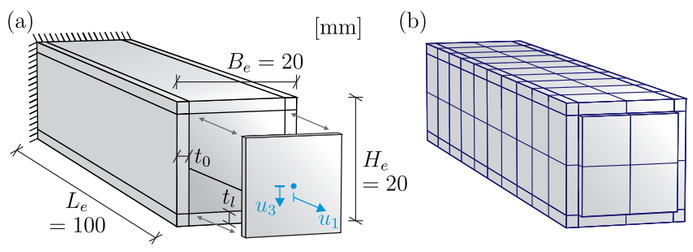

Figure 1: (a) Geometrical design and (b) parametrised FE mesh of a single-chamber SFA.

Using finite element analysis (FEA), the membranes are modelled with 27-node brick elements and exhibit a hyperelastic response described by an Ogden model. The strain-energy function $\Psi(\lambda_1, \lambda_2, \lambda_3)$ is formulated using the m-order power-series approach

$$\Psi_{OG} = \sum_{p=1}^{m} \frac{\mu_p}{\alpha_p} \left(\lambda_1^{\alpha_p} + \lambda_2^{\alpha_p} + \lambda_3^{\alpha_p} - 3 \right) + \kappa \mathcal{G}(J)$$

$$\text{with} \qquad \mathcal{G}(J) = \frac{\Lambda}{4} \left(J^2 - 1 - 2 \ln J \right) - \sum_{p=1}^{m} \mu_p \ln J \,.$$

$\{\lambda_i\}_{i=1,3}$ denote the principal stretches, J the volume ratio, and $\{\mu_p\}_{p=1,m}$, $\{\alpha_p\}_{p=1,m}$, κ, and Λ represent material parameters, e.g. fitted to Treloar's data [2]. When the structure is inflated under positive or negative pressure p_0, it undergoes large deformations. Within FEA, the chamber pressure is represented as a displacement-dependent surface load $\mathbf{p} = p_0(\mathbf{x}) \cdot \mathbf{n}$. If all membranes share a uniform thickness t_0, the resulting deformation mode is termed 'ballooning'.

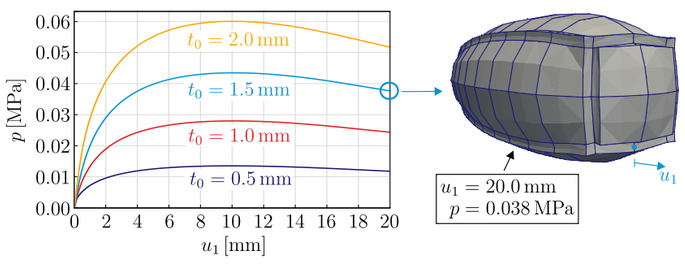

Figure 2: Load-displacement curves of a single-chamber SFA tip for various membrane thicknesses.

The effect of wall thickness variation is illustrated in Figure 2. Since bending capability is central to gripping applications, curvature must be induced. This is achieved by introducing an asymmetric cross-section – e.g., by stiffening or thickening one membrane – as illustrated in Figure 3, where the lower membrane thickness t_l is a multiple of t_0.

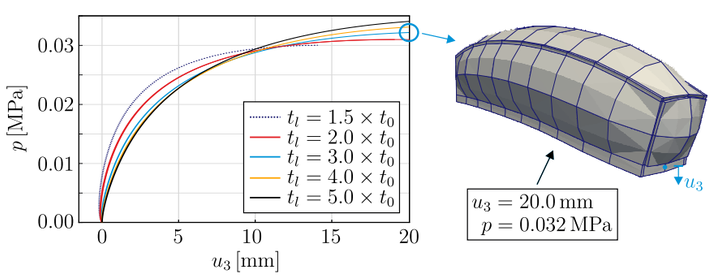

Figure 3: Load-displacement curves of a single-chamber SFA tip with asymmetric cross-section.

Incorporating fibres – whose number and arrangement are discussed in Xavier et al. [3] – suppresses undesired ballooning and enhances bending performance, especially when wrapped radially.

3. The multi-chamber actuator

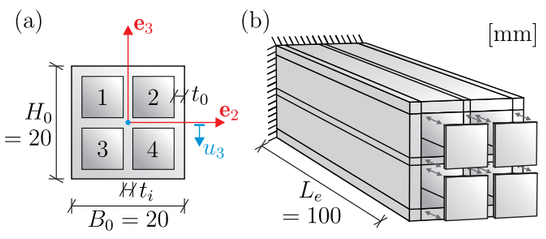

Figure 4: (a) Cross-sectional view and (b) overall view of a four-chambered SFA.

Another possibility to induce bending is the use of multiple chambers (Figure 4). Four chambers $c \in 1,2,3,4$ are arranged in a rectangular configuration. Using a load factor λ and a chamber-specific pressure scale factor ξ_c, each chamber is inflated with an individual positive or negative pressure

$$p_c = \xi_c \cdot \lambda \cdot p_0 \quad \text{with} \quad \xi_c \in [-1, 1] \,.$$

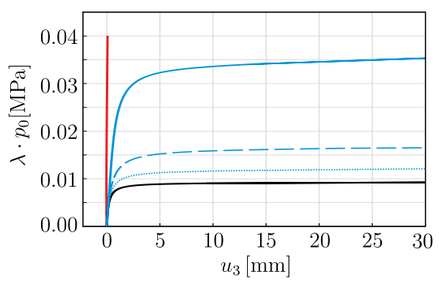

Configuration	ξ_1, ξ_2	ξ_3, ξ_4
B1	0.0	1.0
B2	0.0	−1.0
B3	$\frac{1}{4}$	−1.0
B4	$\frac{1}{2}$	−1.0
B5	1.0	−1.0

Figure 5: Load-displacement curves für multi-chamber SFAs subjected to pressurisation.

Table 1: Values of $\xi_c\,[-]$ for pressure configurations B1-5.

In bending tests (Table 1) for two pressurised chambers 3 and 4, positive pressurisation (B1) yields no bending (Figure 5). Negative pressure (B2) instead, shows excellent bending behaviour, which is consistent with the findings of Ainla et al. [1]. The influence of positive pressurisation in chambers 1 and 2 (B3, B4, and B5) indicates that effective bending can be achieved when $|p_c^-| > 2\,p_c^+$. Analougus findings for biaxial bending modes are made, when one chamber is actuated predominant and the condition $\sum_{c=1}^{4} |p_c^-| > \sum_{c=1}^{4} p_c^+$ is pertained.

4. Experimental investigations

The numerical results can qualitatively be confirmed by the experimental data (Figure 6), especially regarding their highly nonlinear behaviour. Although, a limit of deformation caused by instability of the structure can be observed. Divergences in the magnitude of the resulting displacements may be traced back to model assumptions, e.g. differences in geometrical and material design parameters in both the numerical and the experimental model.

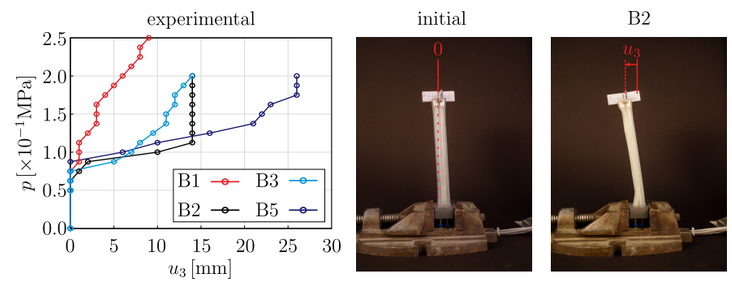

Figure 6: Load-displacement curves and deformed actuator for configuration B2 in experiment.

5. ANN-based control algorithm

For practical use, a prescribed actuator tip displacement cannot be achieved without knowing the corresponding pressure configuration. As the database for the many possible deformation states grow rapidly, employing an artificial neural network (ANN) becomes advantageous. Using 1,000 training samples, it is shown that for a given input $\mathbf{u} = [u_1, u_2, u_3]^T$, a feedforward ANN with two hidden layers of 15 neurons each can accurately predict the required pressures $\mathbf{p} = [p_1, p_2, p_3, p_4]^T$ and reproduce the tip trajectory to an arbitrary point Q (Figure 7). Thus, the ANN can be integrated into a control unit for omnidirectional gripping applications.

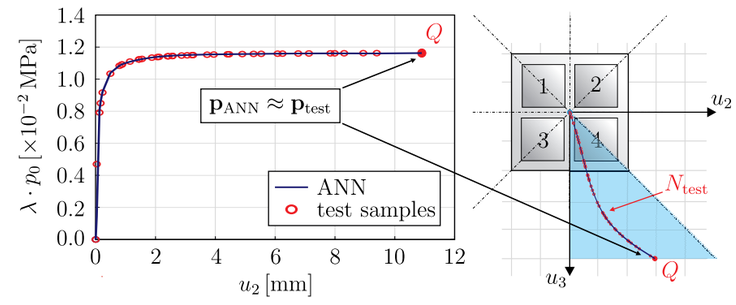

Figure 7: Analytical and ANN-solution for a four-chamber SFA's pressure-displacement relationship.

References

[1] Ainla, A. / Verma, M.S. / Yang D. / Whitesides G.M.: *Soft, Rotating Pneumatic Actuator.* Soft Robotics 4(3) (2017), p. 297–304.

[2] Treloar, L.R.G.: *The Elasticity of a Network of Long-Chain Molecules. II.* Rubber Chemistry and Technology 17(2) (1944), p. 296–302.

[3] Xavier, M.S. / Fleming, A.J. / Yong Y.K.: *Finite Element Modeling of Soft Fluidic Actuators: Overview and Recent Developments.* Advanced Intelligent Systems 3(2) (2020).